Coevolution and temporal dynamics of species interactions shape species coexistence

François Duchenne*[1], Virginia Dominguez-García[1], Francisco P. Molina[1] & Ignasi Bartomeus[1]

[1] *Estación Biológica de Doñana (EBD-CSIC), Sevilla, Spain*

*: *corresponding author, francois.duchenne@wsl.ch*

Keywords: feasibility | emergent properties | morphology | structure | competition | plant | pollinator

Data availability statement:

Codes to perform simulation, to do figures and to analyse empirical networks are available here: https://github.com/f-duchenne/Evolution_pheno_vs_morpho

Empirical plant-pollinator interaction data are available here: https://doi.org/10.5281/zenodo.13270452

Competing Interest Statement:

The authors declare no competing interests.

Author contributions:

FD designed the study and performed all analyses with inputs from VDG and IB. FPM collected the data, with punctual help from IB. FD wrote the first draft and all authors participated to editing and writing the final version.

Abstract

Evolutionary and ecological forces shape species coexistence, but how different ecological mechanisms drive coevolutionary dynamics remains poorly understood. Focusing on mutualistic communities, we explore how morphological and phenological trait matching can shape the coevolution of species traits, influence the evolutionary trajectories at the community level, and determine community stability. Using *in silico* experiments, we first show that because phenological traits can decouple interactions in time, their coevolutionary dynamics led to the emergence of interaction motifs promoting facilitation over competition. In contrast, coevolution driven by morphological traits led to poorly structured networks with higher connectance. As a consequence, phenological coevolution increased the ecological stability of the community, relative to those coevolved based on morphology, and dampened the diversity-stability trade-off observed in morphologically coevolved communities. Next, by using 17 empirical pollination networks, we show that phenological motifs promoting facilitation were abundant in natural communities, and that as predicted by the theoretical models, the phenological structure in species interactions was a major determinant of the structural stability of these empirical communities. These results show that modelling explicitly the basic mechanisms determining species interactions is crucial to understand how species coevolve, and the ecological properties emerging at the community level, such as community structure and stability.

Introduction

The coevolution among organisms interacting mutualistically have fascinated biologists for many centuries (1, 2), but its role in shaping community stability remains unclear (3–5). Over the last decades, the study of mutualistic communities has developed a deep, although mostly theoretical, understanding of the ecological determinants of the community stability (6–12). However, most of this work has been conducted from an ecological perspective, largely neglecting coevolutionary dynamics. Fragmented pieces of evidence show that coevolution can affect species interaction strengths (13, 14), which affects the structure of species interaction networks (15, 16), which is expected to determine community stability (6–9, 17). These works have shown that the outcome of coevolutionary dynamics at community level primary depends on the ecological mechanisms determining species interactions from species traits, *i.e.* linkage rules. Different linkage rules lead to different network structures (15, 16), suggesting that the mechanisms determining species interactions are important for understanding how coevolutionary dynamics affects community stability.

Phenological and morphological matching are the most frequent linkage rules in pollination networks (18, 19) and they exhibit distinctive effects on community stability (20). Morphological and phenological traits can both constrain interaction strength and create forbidden links, which can increase community stability (6, 9). However, while morphological traits structure interactions in a static way, phenological traits lead to dynamic plant-pollinator interactions over time (18, 19, 21, 22). The species turnover created by phenological traits is expected to have a positive effect on community stability, because it can promote facilitation over competition (20) when phenologies are organized in such a way that mutualistic partners overlap in time more than competitors do (Fig. 1a). Thus, we expect that phenological traits might play a bigger role than morphological traits in driving community stability, but only if specific facilitative structures are able to emerge from coevolutionary dynamics. Since evolution is driven by differences in species fitness, it is not clear whether evolutionary dynamics would lead to community-level structures enhancing stability (23).

The few studies that have assessed the effect of coevolutionary dynamics on the stability of mutualistic communities compared to non-coevolved communities show contrasting results, reporting either an increase (24) or a decrease (25) in network persistence, or a decrease in resilience (3, 5) but an increase in robustness to perturbation (4). These contrasting results are not completely incompatible, as different stability metrics can quantify different aspects of the community stability (26, 27). Moreover, even among studies using the same stability metric, results might not be comparable because of different parametrization. Using stability metrics such as persistence and resilience often requires an arbitrary parametrization of growth rates, and then the results hold only for a given combination of growth rates, which limit comparisons among studies. One way to overcome this limitation is adopting an structuralist approach (7), which measures the overall effect of species interactions on the stable coexistence of species, over all possible growth rates (7, 28).

None of the previous studies assessing the effect of coevolutionary dynamics on the stability of mutualistic communities have explicitly incorporated phenology as a potential mechanism structuring species' interactions. Since phenological and morphological traits have distinctive effects on the facilitation-competition balance, we expect that they would lead to divergent evolutionary dynamics, resulting in contrasting emergent properties, such as structure and

stability. However, verbal predictions about evolutionary trajectories in a community context remains difficult to emit, because coevolution is strongly driven by long-path indirect effects and not only by direct interactions (14, 29), requiring the use of dynamical models and *in silico* experiments to obtain predictions that can be otherwise counterintuitive.

To investigate the effect of phenological and morphological traits on the evolutionary dynamics of mutualistic networks and their stability, we first developed a coevolutionary model that we coupled with a structuralist approach to measure community stability (7). Then, we analyzed a set of 17 time-structured empirical plant-pollinator networks and tested if the signal of phenological coevolution could be detected, and we assessed how this seasonal structure affects the structural stability of natural communities. Our results show how incorporating both coevolutionary dynamics and temporal dynamics in community ecology can help to answer the longstanding question of how diverse natural communities can be stable.

Results

In our coevolutionary model each species was characterized by a gaussian trait, with a mean and a variance, and species interaction strengths were defined by the overlap between their gaussian traits. For each simulation, we tracked the trait values, the emerging interaction network structure, and the structural stability of the full community over time. The species' trait was either a phenological trait or a morphological trait. For each of these two scenarios (phenology *vs.* morphology), the two kinds of traits were treated exactly in the same way, and only the calculation of the temporal co-occurrence between species (τ) differed between the two sets of simulations, making our two scenarios perfectly comparable (*cf.* Methods). When considering a phenological trait, temporal co-occurrence was defined by the overlap among phenologies ($0 \leq \tau \leq 1$), while when considering a morphological trait the temporal co-occurrence was set to one, because all interactions happen simultaneously. This temporal co-occurrence (τ) shaped the competition for mutualistic partners: two species compete for a mutualistic partner only if they co-occur in time.

In simulations with phenological traits the proportion of "V" motifs promoting facilitation over competition ("V+" motifs) increased over time, much more than in corresponding simulations with morphological traits (Fig. 1a-b). "V+" motifs did not exist when the trait was a morphological one, because all interactions were simultaneous ($\tau = 1$), which means that if two species shared the same mutualistic partners they also competed for it. However, an equivalent "V" motif could still be computed by treating morphology as phenology for that point of the manuscript only (*cf.* Methods). This proportion of equivalent "V" motif could give us an idea of how these structures could appear spuriously in evolutionary dynamics that are blind to the effect of these motifs. Coevolution driven by phenology produced more "V+" motifs than expected by morphological coevolutionary dynamics that were insensitive to the effects of these "V+" motifs. This pattern was even stronger when performing simulation with lower competition strength (Fig. S1).

The emergence of abundant "V+" motifs when considering phenological coevolution translated into a quick drop of the average competition strength in the community over time (Fig. 1c). Regardless the initial difference in competition values among the two scenarios, a trivial consequence of phenological traits decreasing species temporal co-occurrence, what interested us was how competition strength changed over time, as the coevolution dynamics

unfolded. We observed that competition for mutualistic partners decreased in communities structured by phenological traits, while tended to be stable in those structured by morphology (Fig. 1c). This suggests that phenological coevolution is more likely to decrease the likelihood of competitive exclusion than morphological coevolution. These divergences in motif production and competition strength can be understood by examining the distribution of species traits. Phenological coevolution tended to produce much more specialist species with very fewer generalists than morphological coevolution (Fig. S2).

These first results show that, when considering phenology, coevolutionary dynamics produced patterns that tended to promote facilitation over competition, compared to coevolutionary dynamics driven by morphology.

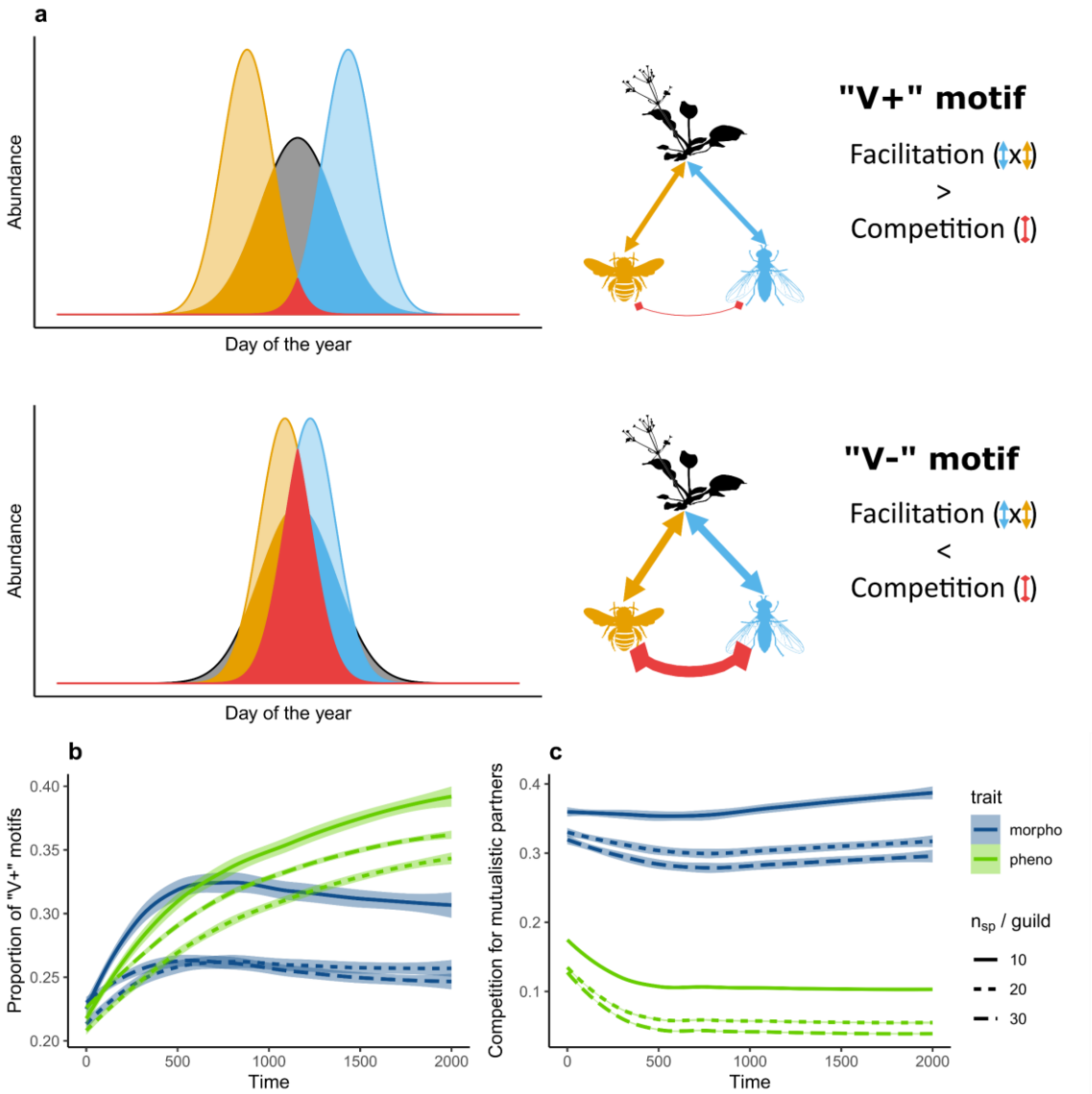

Fig. 1: motifs promoting facilitation emerge from phenological coevolution. *(a) Schematical examples of "V" motifs: on the top a "V" motif promoting facilitation ("V+"), and on the bottom a V motif promoting competition ("V-"). In the top, pollinators interact with the same plant but overlap little in time, and hence they almost do not compete but facilitate each other. The facilitation between pollinators is the positive indirect effect mediated by the plant (the product of the mutualistic interactions). In the bottom pollinators largely overlap in time, a structure which tend to promote competition over facilitation, which can lead to competitive exclusion. (b) Proportion of "V+" motifs, relative to the total number of V motifs as a function of time, diversity (number of species per guild) and trait. Morphological*

coevolution gives the proportion of "V+" motifs that emerge spuriously from trait reorganization (cf. Methods). (c) Average competition strength as a function of time, diversity and kind of trait showing that phenological traits have an initial decrease in competition, while morphological traits are stable, and if anything increase. In (b) and (c) the lines and ribbon show the estimated values and their 95% confidence interval, respectively, obtained by a locally estimated scatterplot smoothing (LOESS) of the values across time.

Our simulations showed that in addition to these specific motifs, phenological and morphological coevolution led to highly divergent evolutionary trajectories across various aspects of network structure, such as connectance and nestedness (Fig. 2 & S3). These divergences were so marked that there was almost no overlap in the final outputs (Fig. 2a-c). Phenological coevolution led to more nested and less connected interaction networks than morphological coevolution (Fig. 2d-e). As these two components are key determinants of the stability of mutualistic communities (6–8, 17), we can anticipate that phenological and morphological coevolution will shape community stability in very different ways. Communities shaped by phenological coevolution, which tend to be more nested and less connected, are expected to be more stable than those shaped by morphological evolution.

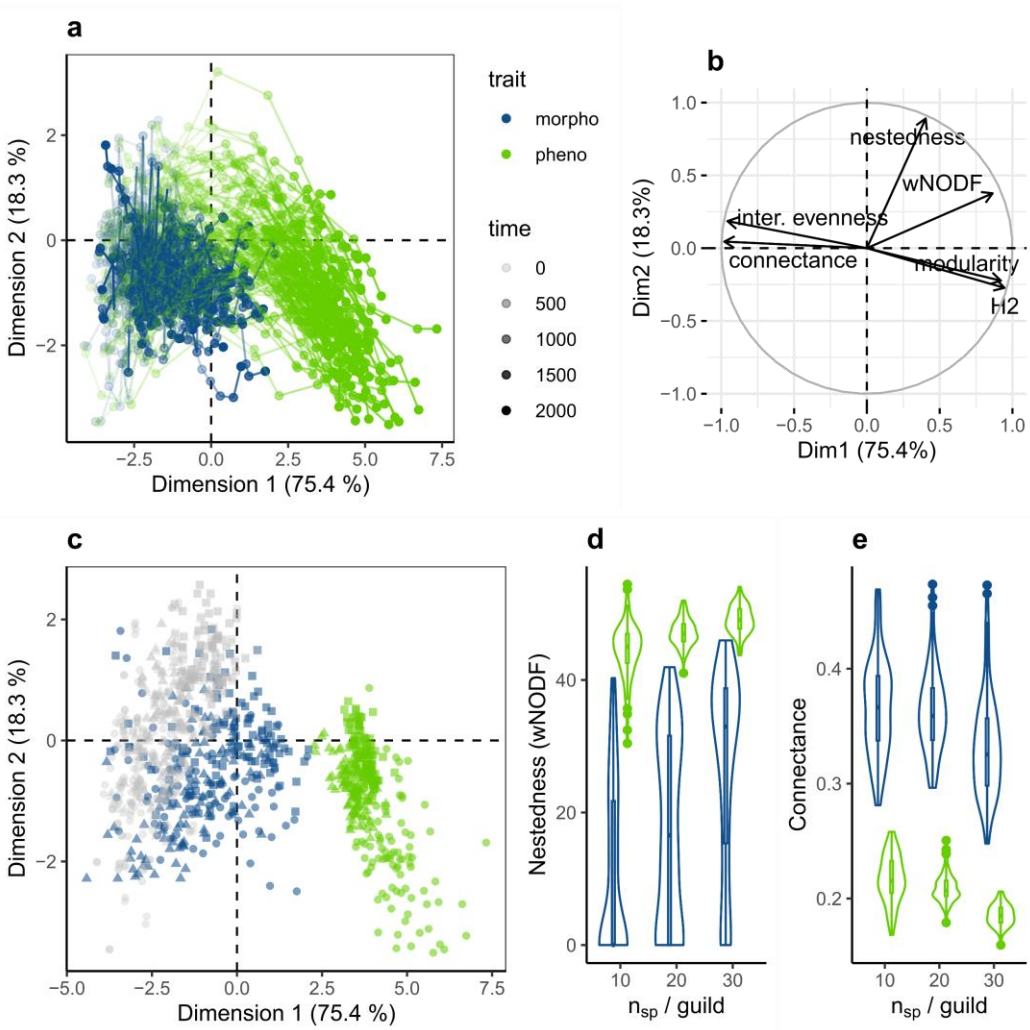

Fig. 2: phenological and morphological coevolution led to divergent evolutionary trajectories of communities. *(a) Location of each network at different time steps, in a multidimensional space of network structure. The multidimensional space of network structure was created using the Principal Component Analysis (PCA) illustrated in (b). Here only the simulations with 10 species per guild are represented for readability. (b) PCA loading plot, where wNODF is a weighted measure of nestedness*

and H2 a measure of specialisation (cf. methods). (c) Final location of each community in the multidimensional space of network structure (coloured points) relative to initial locations (grey points). Circles represent simulations with 10 species per guild, triangles 20 species per guild and squares 30 species per guild. (d) and (e) represent the nestedness (measured as wNODF) and the connectance of the final networks, as a function of the number of species per guild and kind of trait. Simulations performed with a competition strength of c =10.

To measure the stability of our mutualistic communities, we use the concept of structural stability, which represents the average probability that any given species in the community persists in time (7, 17, 30). Our simulations show that the structural stability of the communities (ω) strongly diverge over evolutionary time between communities structured by phenology and morphology (Fig. 3).

The initial structural stability was higher for communities structured by phenology (Fig. 3), because decoupling interactions in time, even randomly, decreases competition strength (Fig. 1c). However, what most interested us was seeing how coevolution shaped it, *i.e.* the trajectory over time of this structural stability. In a context of moderate or high interspecific competition, phenological evolution strongly increased structural stability, while morphological evolution did not have a clear effect (Fig. 3). However, note that this trajectory depended on the strength of the interspecific competition relative to the intraspecific competition, fixed by the parameter ρ. Hence, in the context of a very low interspecific competition, the coevolutionary dynamics affect weakly the structural stability because the stability of the community is mostly driven by intraspecific competition (Fig. S4).

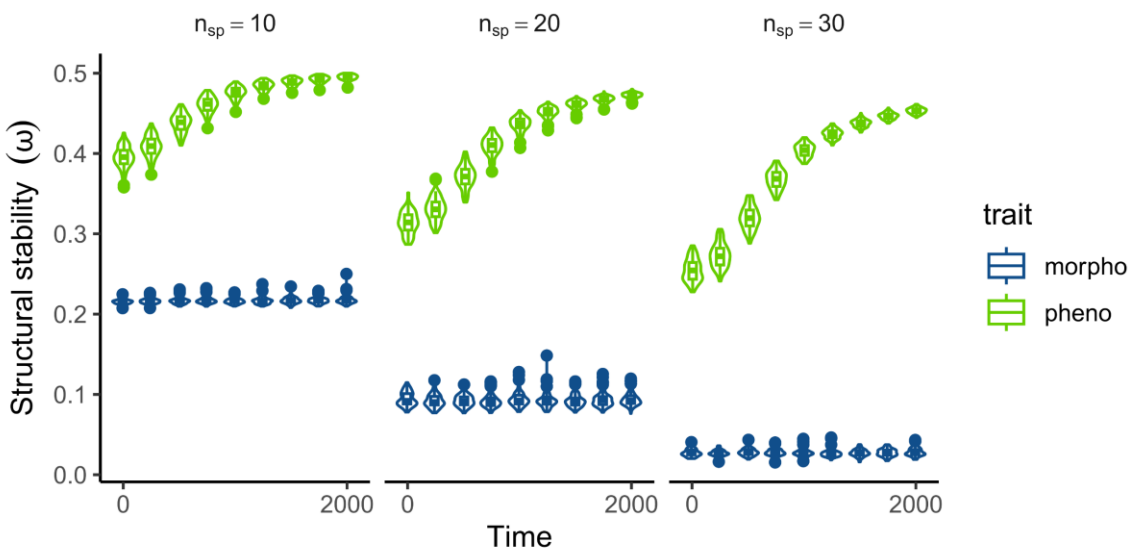

Fig. 3: phenological coevolution increased structural stability and dampened the diversity-stability trade-off. *Changes in structural stability (average persistent probability) over time, for the two evolutionary scenarios and number of species per guild, when interspecific competition was relatively strong (ρ = 0.4). Simulation performed with an overall competition strength c = 10, see Fig. S5 for simulations with c = 5. The x-axis is square-root transformed.*

Importantly, in a context of realistic moderate to high interspecific competition, phenological coevolution also dampened the diversity-stability trade-off (Fig. 4). At initial conditions, the number of species per guild negatively affected the structural stability (Fig. 4a), which is a known relationship (31). However, in networks coevolved based on a phenological trait this relationship was barely visible, the structural stability being similar across different diversity values at the end of the simulations (Fig. 4b). In contrast, the diversity stability trade-off was still strong in coevolved networks when considering a morphological trait (Fig. 4b). This result suggests that coevolutionary dynamics can dampen the diversity-stability trade-off, when considering phenological coevolution but not when considering morphological coevolution.

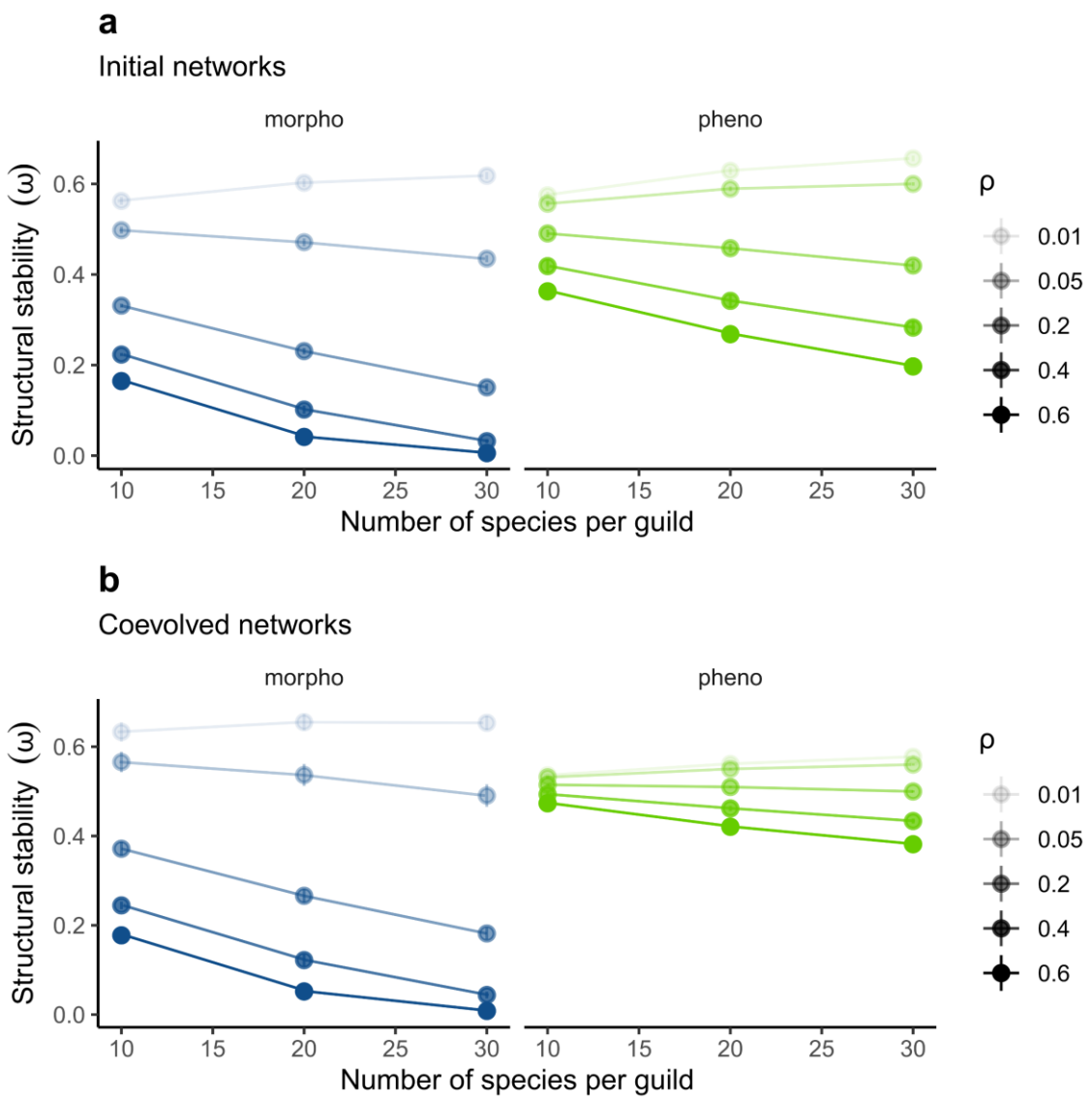

Fig. 4: Coevolution of phenologies dampened the diversity-stability trade-off. *Structural stability as a function of the number of species per guild (i.e. diversity), the evolutionary scenario (morphology vs phenology) and the interspecific competition strength (ρ), for (a) initial and (b) coevolved networks. We represented the average value ± the standard deviation (error bars are almost always too small to be visible). Simulations performed with a competition strength c = 10.*

Finally, to assess the stabilizing role of phenology on real-world communities, we analyzed the phenological organization of 17 empirical plant-pollinator networks (cf. Table S1). We found evidence for a high proportion of the "V+" motifs (Fig. 5a), described in Fig. 1a, which

were predicted by our model to be abundant in a context of phenological coevolution. Performing coevolutionary simulations with networks having the same number of species per guild as the empirical ones (*cf.* Methods), we show that the motif promoting facilitation were slightly less abundant in real networks than in simulations with phenological coevolution, but more abundant than what would emerge spuriously from morphological coevolution (Fig. 5a). It is also worth noting that the overall structure of the empirical networks was better reproduced by simulations with phenological coevolution than by simulations with morphological coevolution (Fig. S6).

We assessed the structural stability of empirical communities by either considering that all interactions were simultaneous (*i.e.* aggregated networks) or considering the observed seasonal structure in interactions (*cf.* Methods). As predicted by the simulations, considering the seasonal structure in interactions led to an increase in the structural stability of the empirical communities (Fig. 5b-c). This shows that the stabilizing role of the coevolved seasonal structures that we found *in silico* is likely to be important in stabilizing natural mutualistic communities. The positive effect of the seasonal structure on the structural stability increased with species diversity, which means that the seasonal structure was dampening the diversity-stability trade-off (Fig. 5b). This positive effect also increased with the strength of the interspecific competition (ρ, Fig. 5c), suggesting that seasonal structures might be of particular importance in diverse communities and when competition for mutualistic partners is strong.

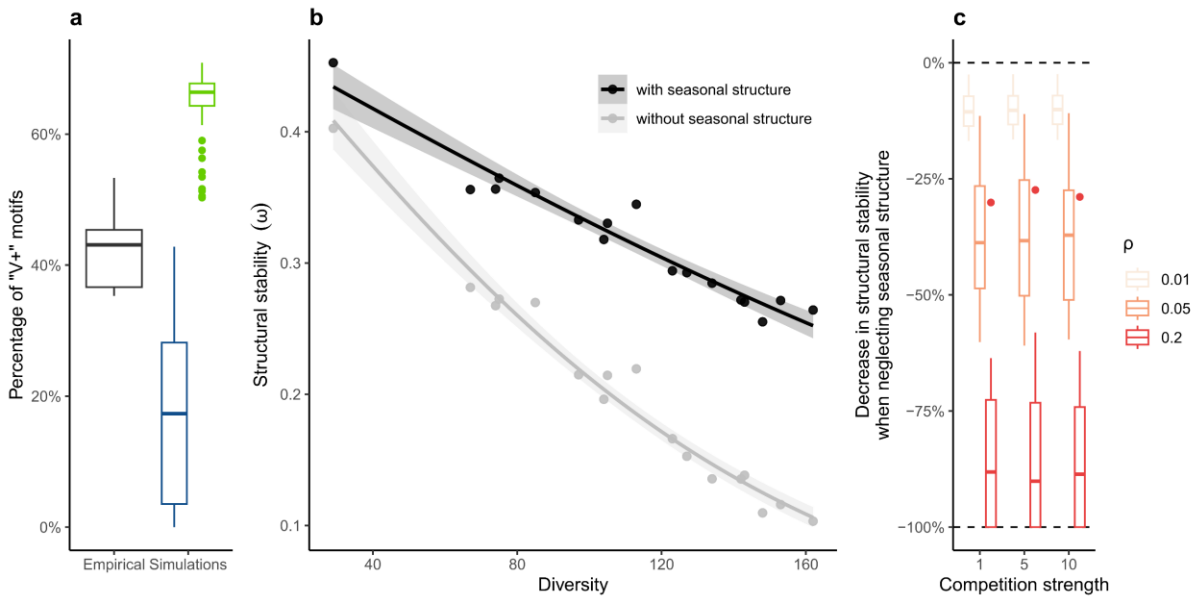

Fig. 5: Seasonal structure in interactions stabilize natural communities. *(a) Distribution of the percentage of "V+" motifs, relative to the total number of V motifs, in the 17 empirical networks, and in simulated coevolved networks with similar dimensions (cf. methods), using phenological coevolution (green) or morphological coevolution (blue). (b) Structural stability, average probability of persistence, as a function of community diversity (number of pollinator and plant species), when accounting for seasonal structure in competitive interactions or when neglecting this seasonal structure. For a given overall competition and interspecific competition strengths (c = 5 & ρ = 0.05). The lines and ribbon show the estimated values and their 95% confidence interval, respectively, obtained by generalized linear model with a quasi-binomial error structure. (c) The decrease in percentage of the structural stability observed when neglecting seasonal structure, relative to the measure when considering it, as a function of the overall competition strength (c parameter, cf. Methods) and of the interspecific competition strength (ρ, cf. Methods). n = 17 for each boxplot. Dots represent outliers.*

Discussion

Our results show that explicitly modelling the linkage rules defining species interactions is important to understand the community level outcomes of coevolutionary dynamics. Using an integrative metric of ecological stability, we show that the structural stability of mutualistic communities was enhanced by phenological coevolution but was diminished by morphological coevolution. Our results highlight that a largely neglected ecological mechanism, the temporal organization of species interactions that emerges when phenological traits are considered, is key to understand coevolutionary dynamics and the stability of diverse mutualistic communities.

Phenological traits can decouple interactions in time, rendering an asymmetric partition between the mutualistic interactions and the competition for mutualistic partners (20, 32), in contrast to morphological traits. Surprisingly, this key mechanism for species coexistence has only recently been integrated to ecological models, but is now well recognized (10, 20, 33–36). However, the emergence from coevolutionary dynamics of seasonal structures fostering stability remained uncertain. Here we show that these community level patterns can emerge naturally from species fitness driven coevolution. In contrast, when considering only morphological traits, the coevolutionary dynamics only slightly diverged from the initial random structures. Thus, ecological mechanisms determining species interactions (*i.e.* linkage rules) influence the coevolutionary outcomes at community levels, that in return determines the ecological stability of the community. This successive effects between ecological and evolutionary mechanisms suggest that developing eco-evolutionary models combining simultaneous ecological and evolutionary dynamics is a promising future step to understand the role of coevolution in determining community stability (37).

The outcome of coevolutionary dynamics strongly depended on competition for mutualistic partners, which is highly consistent with what we know from the ecological dynamics of mutualism (6, 38). In a context where interspecific competition was low, we observed a positive diversity-stability relationship, in both non-coevolved and coevolved communities. This is because more species imply more mutualistic interactions, which translate in more benefits for species and thus a higher persistence. However, when considering a more realistic scenario of moderate or high interspecific competition (12), the diversity-stability relationship turned negative, as expected from the longstanding diversity-stability debate (26, 39). This is because mutualism generate competition for mutualistic partners, and thus increase the likelihood of competitive exclusion of at least a few species. In this context, phenological coevolution dampened the diversity-stability trade-off, while morphological coevolution did not. Interspecific competition for mutualistic partners has been reported to be strong in many different mutualistic systems: pollination (40), seed-dispersal (41, 42), mycorrhizae (43), cleaner-client fishes (44), etc. According to our results we expect that these systems would exhibit a strong seasonal structure in interactions.

Importantly, our model did not include any abiotic constrain on phenologies other than physiological bounds. Thus, in our simulations, the emergence of seasonal structure was only driven by species interactions. This suggests that the mechanism we describe is universal: seasonal structures in interactions are expected to be present in every mutualistic system where interspecific competition for mutualistic partners is high enough, regardless the abiotic seasonality. It could explain why even tropical mutualistic systems with relatively constant

abiotic conditions, such as plant-hummingbird interactions, exhibit a strong seasonal structure (19), that increases community stability relative to hypothetic cases without or with random seasonal structure (35).

Merging theory and empirical data is important to determine the importance of possible mechanisms hinted by theory, in shaping species coexistence in nature. Using a set of 17 empirical networks, we found phenological motifs promoting facilitation in a higher proportion than what would emerge spuriously from other coevolutionary dynamics, suggesting that observed seasonal structures have been shaped by phenological coevolution, at least partially. It is however important to note that we found a lower proportion of these motifs than expected by purely phenological coevolution, which can be explained by the fact that morphological coevolution interplays with phenological coevolution, leading to an intermediate output. It might also be due to abiotic conditions constraining species phenologies (45) potentially blurring the effect of coevolution. Nerveless, neglecting the seasonal structure in interactions, and thus these motifs promoting facilitation, could lead to underestimating the structural stability of the empirical communities from ~10% to 100% depending on the community diversity and interspecific competition strength.

By showing that complex and collective structures fostering stability can emerge from species' fitness driven evolution, we effectively link coevolutionary mechanisms and community ecology. Most importantly, the emergence of these stabilizing structures depends on which kind of traits coevolve: while coevolution of morphological traits does not increase community stability, coevolution of phenologies tends to do so and dampen the diversity-stability trade-off. Overall, our results suggest that coevolutionary dynamics enhance the positive effect of seasonal structures on community stability (10, 20, 33–35), which is probably a key mechanism to understand how natural communities can be both diverse and stable.

Methods

Our model describes the evolution of a gaussian trait, for each species embedded in a community, all species coevolving together. For simplicity we took the example of a plant-pollinator community, but the model could apply to any mutualistic community.

Species trait

Each species was characterized by a trait with a mean (μ) and standard deviation (σ). Both parameters of the trait evolved independently, *i.e.* we assumed no genetic covariance among them. To make comparisons possible between simulations with a morphological or a phenological trait, both traits were treated exactly in the same way, on a scale that goes from 0 to 365. For phenology it obviously recalls the day of the years, while for morphology it can be any abstract scale.

To mimic physiological limits, we bounded the mean trait values between 80 and 285, and the standard deviation values from 1 to 50. To bound trait values without using a sharp truncation that would create weird behaviors at the bounds, we used a process inspired by generalized linear models, in which the trait evolves on an unbounded latent distribution linked to the effective bounded values through a link function. As a link function we used a modified logit function (cf. Supplementary Methods I). In the following part, μ and σ, denote the values on the bounded scale (real mean and standard deviation), while $\ddot{\mu}$ and $\ddot{\sigma}$ denote the value on the latent unbounded scale. For example, $\ddot{\mu}$ varied from $-\infty$ to $+\infty$, but μ was bounded between 80 and 285.

Species interactions

The overlap between the traits of a pollinator j and a plant i defined the strength of the mutualistic interaction between them. To calculate the overlap, we used the area below the minimum of the two gaussian traits involved (Fig. 1a):

$$\gamma_{ij} = \int_0^{365} min\left(\frac{1}{\sigma_i\sqrt{2\pi}} e^{\frac{-1}{2}\left(\frac{x-\mu_i}{\sigma_i}\right)}, \frac{1}{\sigma_j\sqrt{2\pi}} e^{\frac{-1}{2}\left(\frac{x-\mu_j}{\sigma_j}\right)}\right) dx \quad (1)$$

This means that the mutualistic interaction strengths are bounded between zero and one ($0 \leq \gamma_{ij} \leq 1$), which is convenient as their multiplication would lead to values remaining inside that interval.

The competitive effect (α_{ik}) of a plant k on a plant i, was defined by the product of their interaction strength on shared partners, divided by the total amount of mutualistic interactions of plant i. This led to an asymmetric competition matrix, where specialist species were more sensitive to competition for their partners than generalists. The competition coefficient were calculated as follow:

$$\alpha_{ik} = \tau_{ik} \frac{\sum_{j=1}^{n_A} \gamma_{ij}\gamma_{kj}}{\sum_{j=1}^{n_A} \gamma_{ij}} \quad (2)$$

where n_A was the number of pollinator species, and τ was an index of co-occurrence in time modulating competition. If the trait was a morphological trait, all interaction happened simultaneously ($\tau_{ik} = 1$), and if the trait was a phenological trait, τ_{ik} was the phenological

overlap between plant k and plant i calculated similarly to the overlap between mutualistic partners:

$$\tau_{ik} = \int_0^{365} min\left(\frac{1}{\sigma_i\sqrt{2\pi}} e^{\frac{-1}{2}\left(\frac{x-\mu_i}{\sigma_i}\right)}, \frac{1}{\sigma_k\sqrt{2\pi}} e^{\frac{-1}{2}\left(\frac{x-\mu_k}{\sigma_k}\right)}\right) dx \quad (3)$$

Importantly, the calculation of τ was the only difference between the simulations in the morphological or phenological scenario. When the trait was phenological, two species competed for a partner only if they interacted with it at the same time.

We set the intraspecific competition to one, $\alpha_{i,k=i} = 1$, to ensure diagonal dominance of our system. The competition coefficient among pollinator species was calculated with an equation similar to equation (2).

Species fitness and trait evolution

To compute trait evolution, we needed a fitness measure to infer in which direction traits will evolve. To do so, we defined the fitness of species i (W_i) as the balance between competition and mutualism, which can positive or negative:

$$W_i = -c\sum_{k=1}^{n_P} \alpha_{ik} + \sum_{j=1}^{n_A} \gamma_{ij} \quad (4)$$

where c is the overall strength of the competition, relative to mutualism. Thus, the direction of selection imposed by species interaction on a trait parameter was defined by the partial derivative $\frac{W}{\partial \ddot{\mu}_i}$. According to that, $\ddot{\mu}_{i,t}$ was defined as:

$$\ddot{\mu}_{i,t} = \ddot{\mu}_{i,t-1} + \varepsilon \frac{W}{\partial \ddot{\mu}_i} \quad (5)$$

where ε is a parameter controlling evolution speed, which can relate to genetic variance. Since our fitness measure was based on a linear equation, it can exhibit very sharp fitness gradient and to avoid evolutionary jump we truncated the values of $\frac{W}{\partial \ddot{\mu}_i}$ to [-5,5]. $\ddot{\sigma}_{i,t}$ was calculated with an equation similar to equation (5).

Simulations

We performed simulations over 2000 time steps. In our time-discrete model, traits values never reach an equilibrium because all species traits change simultaneously, but the trait evolution was fast in the first 200 steps, before slowing down (Fig. S7), leading to very minor structural changes after that (Fig. S8). We performed simulations over a set of 100 random initial combinations of traits values. We drew initial trait values on the modified logit scale (*cf.* Supplementary Methods I) from a uniform distribution for the mean and the standard deviation: $\ddot{\mu}_{i,t=0} \sim U(-2.5,2.5)$ and $\ddot{\sigma}_{i,t=0} \sim U(-2.5,2.5)$.

We generated 100 initial conditions for 3 different values of initial diversity: 10, 20 and 30 species per guild. For each initial condition, the simulation was run twice, considering a morphological trait ($\tau_{ik} = 1$), or a phenological trait ($\tau_{ik} \sim$ equation (3)).

Our simulations required very few parameterizations, because most of the coefficients were determined by the evolving trait values. However, we needed to choose a value for competition strength, the parameter c in equations (4) and (6). Since our competition coefficients are always smaller than the mutualistic interaction strength (*cf.* equation (2)), we needed a high value of c to avoid mutualistic orgies, a common behaviour in linear models of mutualistic communities (46). A mutualistic orgy would lead to get all the species quickly converging to the same trait value and would thus not be realistic. In the main text, we presented the results for simulations performed with $c = 10$, and we also presented results with $c = 5$ in supplementary materials (Fig. S1, S3 & S4). Results remained the same over a wide range of values.

Motifs promoting facilitation

To test if co-evolutionary dynamics can lead to phenological motifs that promote facilitation over competition, we calculate the number of motifs with a "V" shape promoting facilitation, or "V+" motifs (Fig. 1a). This kind of motifs can be present only in the phenological scenario. In contrast, when considering morphological traits, all interactions happen simultaneously ($\tau = 1$) and thus competition between two species from the same guild does not depend on their trait overlap but only depends on their overlap in mutualistic interactions. However, we calculated an equivalent τ in the morphological scenario using equation (3) and treating morphology as phenology, to evaluate the amount of "V+" motifs that could emerge spuriously. In this case, morphological coevolution thus shows how a reorganization of phenologies driven by a coevolutionary process blind to the "V+" motifs still may generate them by chance.

Since our in-silico mutualistic networks were weighted and without real zeros, we had to put a threshold above which we consider mutualistic interactions were strong enough to constitute "V" shape motifs. We used only the links for which $\gamma > 0.01$ and we extracted all corresponding "V" motifs. We calculated the number of "V+" motifs as those where the two species from the same guild overlapped less in their trait value than the product of their overlap with their mutualistic partner. For example, a "V" motif in which a plant i interact with pollinators j and k would be "V+" motif if $\gamma_{ij}\gamma_{ik} > \tau_{jk}$, and "V-" motif otherwise (see Fig. 1). As connectance was changing among simulations because of different initial conditions, and within simulations, because of coevolutionary dynamics, we estimated the proportion of "V+" motifs, over the total number of motifs with a "V" shape. This allowed to get comparable measures over time and across simulations.

Since evolution slowed down with time (Fig. S7), we measured the proportion of "V+" motifs at different time steps, that were evenly distributed on square-rooted time scale (t = 0, 30, 130, 280, 500, 780, 1130, 1530, 2000).

Network structure

To assess how coevolutionary dynamics affect the structure of the interaction network, we measured indices describing the mutualistic interaction network, at the same time steps that we measured the proportion of motifs promoting facilitation (*cf.* above). We measured connectance, nestedness, modularity, specialisation and interaction evenness. As different indices gave different information, we measured nestedness using two different indices, the index proposed by Galeano *et al.* (47) and the wNODF (48). All these indices were computed with the *bipartite* R package (49).

Structural stability

To understand how evolutionary dynamics affect the ecological stability of our system, we measured the community structural stability. Structural stability is a measure of ecological stability that aims to quantify the range of environmental conditions, modelled through the per capita growth rates (*r*), in which all species can coexist in a stable way (7, 8, 28). The range of environmental conditions, or growth rates, in which all species can coexist is call the feasibility domain, and the structural stability is quantified as the size of the feasibility domain scaled by the number of species in the community, which gives an average measure of species persistence.

The structural stability framework is based on the Lotka-Volterra formalism of population dynamics. The fitness function we used for computing coevolution was similar to the equation of a linear generalized Lotka-Volterra model if all abundances had been fixed to one. The corresponding generalized Lotka-Volterra model, describing variation in the population size of plant *i*, would be:

$$\frac{dN_i}{dt} = N_i\left(r_i - c\sum_{k=1}^{n_P}\alpha_{ik}N_k + \sum_{j=1}^{n_A}\gamma_{ij}N_j\right) \tag{6}$$

where r_i was the per capita growth rate of species *i*. The variation in population size of pollinators was described by a similar equation.

Since the structural stability metric already accounts for competition for mutualistic partners via matrix multiplication and inversion (30), for competition coefficients we used a mean field structured by phenological overlap: $\alpha_{ik} = \tau_{ik}\rho$, where ρ is the interspecific competition strength. For morphological traits all interactions occur simultaneously, $\tau_{ik} = 1$, recovering the classic mean field. As before, we set $\alpha_{i,k=i} = 1$, and we calculated structural stability for different values of the interspecific competition $\rho \epsilon$ [0.01,0.05,0.2,0.4,0.6].

The vector of species abundances at equilibrium (N^*) was given by $N^* = A^{-1}r$, where r was the vector of species growth rates and A was the adjacency matrix describing within guild interaction (competition) as well as between guilds interactions (mutualism) among all pairs of species. This matrix was composed by four blocks:

$$A = \begin{bmatrix} \alpha_{(P)} & -\gamma \\ -\gamma^T & \alpha_{(A)} \end{bmatrix} \tag{7}$$

where $\alpha_{(P)}$ was the competition matrix among plants, dimensions of $n_P \times n_P$, and $\alpha_{(A)}$ was the competition matrix among pollinators ($n_A \times n_A$). γ was the mutualistic interaction matrix ($n_P \times n_A$), and γ^T its transposed.

The feasibility domain is the range of vectors r that give N^* with positive species' abundances only. The size of the feasibility domain ($\Omega(A)$), was calculated as follow:

$$\Omega(A) = \frac{vol\left(D_f(A) \cap B^S\right)}{vol(B^S)} \tag{8}$$

where $D_f(A)$ was the feasibility domain of A and B^S was the closed unit ball in dimension $S = n_P + n_A$.

To quantify structural stability, we normalized the size of the feasibility domain by the number of species in the community: $\omega(A) = \Omega(A)^{1/S}$. The normalized feasibility, $\omega(A)$, is bounded between 0 and 1 and corresponds to the average species persistence probability in the community, represented by the interaction matrix A. The closer the feasibility is to one, the more likely is that all species will coexist in a stable way. To compute this normalized feasibility, we used the *Omega* R function provided by Song *et al.* (28).

Analyses of empirical plant-pollinator interaction networks

We used a set of 17 time-structured plant-pollinator interaction networks, sampled in the area of the Doñana National park, near Sevilla, in Spain, with the protocol described in *ref.* (17). These networks have been sampled at bi-weekly intervals during the peak season (February to May), for one to 8 years (Table S1). Interactions have been recorded at each sampling occasion along a 100m transect during 30 effective minutes, and flower abundances per species have also been recorded along that transect in a standardized way (17). To calculate the structural stability of the empirical networks, we ideally want to get mutualistic interaction strengths that do not depend on sampling effort, neither on species abundances. To correct interaction strength by sampling effort, we calculated the average number of detected interaction per sample round: $\overline{I_{ij}} = \frac{1}{N}\sum_{s=1}^{N} I_{ijs}$, where N is the number of sampling events, and I_{ijs} the number of interactions detected between plant i and pollinator j during sampling event s. To account for species abundances, we divided the average number of interactions by the geometric mean of the marginal sums of species involved in the focal interaction:

$$\gamma_{ij} = \frac{\overline{I_{ij}}}{\sqrt{\sum_{i=1}^{n_P} \overline{I_{ij}} \times \sum_{j=1}^{n_A} \overline{I_{ij}}}} \tag{9}$$

If evolution of phenologies drove, at least partially, the seasonal organization of the interactions, we expect to find a non-negligible proportion of "V+" motifs (Fig. 1a), in line with what we found in coevolved seasonal structures. To do so, we estimated species phenologies. Since sites were all in the same geographical region (maximal pairwise distance was 53km), we assumed that phenologies were the same in all sites and thus we used all the data available to infer phenological parameters, which allows to get more precise phenological estimates per species. We also assumed gaussian phenologies for all species, meaning that we had to estimate only two parameters, the mean and the standard deviation (cf. Supplementary Methods II).

Once we have estimated the species phenologies, we count the number of "V+" motifs, in which the (geometric) average overlap between mutualistic partners was higher than the overlap between the two competitors. To get a measure comparable with our simulations and among networks, as before, we estimated the proportion of "V+" motifs over the total number of "V" shape motifs.

Finally, to see how considering the seasonal structure in interactions affected the structural stability of these communities, we estimated the feasibility (ω) with and without considering the seasonal structure in the interactions. This seasonal structure did not affect the mutualistic interactions (γ_{ij}), as they already depended on phenologies, but only the mean field of competition, which was calculated as in the simulations with $\alpha_{ik} = \tau_{ik}\rho$, and $\alpha_{i,k=i} = 1$. As in simulations, to neglect the seasonal structure in interactions we set $\tau_{ik} = 1$, and to include the

seasonal structure in interactions we calculated τ_{ik} according to equation (3) while using empirical phenologies. We used the generalized linear Lotka-Volterra from equation (6) to calculate the structural stability of the community, with and without seasonal structure in interactions in the same way as described previously, for different values of c and different values of ρ (Fig. 5).

Simulations with empirical networks dimensions

Finally, to compare the structure of the empirical networks with the structure obtained by phenological and morphological coevolution, we performed a new set of simulation using the number of plant and pollinator species, of the empirical networks. We performed these simulations with c = 10, for a set of 10 different random initial conditions (traits values) for each of the 17 empirical networks.

Acknowledgements

We thank Nerea Montes for the help while collecting data. We also thank the taxonomists L. O. Aguado and T. Wood for their help with some bee identifications. FD was funded by *postdoc Mobility* grant from the SNF (project number: P500PB_217801), and VDG by a Marie Skłodowska-Curie grant (N°101064340) from the European Union's Horizon 2021 research. Data collection was funded by a Marie-Curie Career Integration from the European Union's Horizon 2020, the BeeFUN project (PCIG 14-GA-2013-631653), granted to IB.

References

1. C. Darwin, On the Various Contrivances by which British and Foreign Orchids are fertilised by Insects, and on the good effects of intercrossing ... With illustrations (John Murray, 1862).

2. E. I. Jones, J. L. Bronstein, R. Ferrière, The fundamental role of competition in the ecology and evolution of mutualisms. Annals of the New York Academy of Sciences **1256**, 66–88 (2012).

3. N. Loeuille, Influence of evolution on the stability of ecological communities. Ecology Letters **13**, 1536–1545 (2010).

4. S. L. Nuismer, B. Week, M. A. Aizen, Coevolution Slows the Disassembly of Mutualistic Networks. The American Naturalist **192**, 490–502 (2018).

5. S. Suweis, F. Simini, J. R. Banavar, A. Maritan, Emergence of structural and dynamical properties of ecological mutualistic networks. Nature **500**, 449–452 (2013).

6. U. Bastolla, et al., The architecture of mutualistic networks minimizes competition and increases biodiversity. Nature **458**, 1018–1020 (2009).

7. R. P. Rohr, S. Saavedra, J. Bascompte, On the structural stability of mutualistic systems. Science **345** (2014).

8. S. Saavedra, R. P. Rohr, J. M. Olesen, J. Bascompte, Nested species interactions promote feasibility over stability during the assembly of a pollinator community. Ecology and Evolution **6**, 997–1007 (2016).

9. E. Thébault, C. Fontaine, Stability of Ecological Communities and the Architecture of Mutualistic and Trophic Networks. Science **329**, 853–856 (2010).

10. F. Encinas-Viso, T. A. Revilla, R. S. Etienne, Phenology drives mutualistic network structure and diversity: Effects on the dynamics of mutualistic networks. Ecology Letters **15**, 198–208 (2012).

11. C. Song, R. P. Rohr, S. Saavedra, Why are some plant–pollinator networks more nested than others? Journal of Animal Ecology **86**, 1417–1424 (2017).

12. I. Bartomeus, S. Saavedra, R. P. Rohr, O. Godoy, Experimental evidence of the importance of multitrophic structure for species persistence. PNAS **118** (2021).

13. L. P. Medeiros, G. Garcia, J. N. Thompson, P. R. Guimarães, The geographic mosaic of coevolution in mutualistic networks. Proc. Natl. Acad. Sci. U.S.A. **115**, 12017–12022 (2018).

14. P. R. Guimarães, M. M. Pires, P. Jordano, J. Bascompte, J. N. Thompson, Indirect effects drive coevolution in mutualistic networks. Nature **550**, 511–514 (2017).

15. C. S. de Andreazzi, J. Astegiano, P. R. Guimarães Jr., Coevolution by different functional mechanisms modulates the structure and dynamics of antagonistic and mutualistic networks. Oikos **129**, 224–237 (2020).

16. S. L. Nuismer, P. Jordano, J. Bascompte, Coevolution and the Architecture of Mutualistic Networks. Evolution **67**, 338–354 (2013).

17. V. Domínguez-Garcia, F. P. Molina, O. Godoy, I. Bartomeus, Interaction network structure explains species' temporal persistence in empirical plant–pollinator communities. Nat Ecol Evol **8**, 423–429 (2024).

18. P. J. CaraDonna, et al., Interaction rewiring and the rapid turnover of plant–pollinator networks. Ecology Letters **20**, 385–394 (2017).

19. J. Sonne, et al., Ecological mechanisms explaining interactions within plant–hummingbird networks: morphological matching increases towards lower latitudes. Proceedings of the Royal Society B: Biological Sciences **287**, 20192873 (2020).

20. F. Duchenne, C. Fontaine, E. Teulière, E. Thébault, Phenological traits foster persistence of mutualistic networks by promoting facilitation. Ecology Letters **24**, 2088–2099 (2021).

21. J. A. Elzinga, et al., Time after time: flowering phenology and biotic interactions. Trends in Ecology & Evolution **22**, 432–439 (2007).

22. N. de Manincor, et al., Does phenology explain plant–pollinator interactions at different latitudes? An assessment of its explanatory power in plant–hoverfly networks in French calcareous grasslands. Oikos **129**, 753–765 (2020).

23. R. P. Rohr, N. Loeuille, Effects of evolution on niche displacement and emergent population properties, a discussion on optimality. Oikos **2023**, e09472 (2023).

24. F. S. Valdovinos, P. M. de Espanés, J. D. Flores, R. Ramos-Jiliberto, Adaptive foraging allows the maintenance of biodiversity of pollination networks. Oikos **122**, 907–917 (2013).

25. A. Mougi, Stability of an adaptive hybrid community. Sci Rep **6**, 28181 (2016).

26. A. R. Ives, S. R. Carpenter, Stability and Diversity of Ecosystems. Science **317**, 58–62 (2007).

27. S. Kéfi, et al., Advancing our understanding of ecological stability. Ecology Letters **22**, 1349–1356 (2019).

28. C. Song, R. P. Rohr, S. Saavedra, A guideline to study the feasibility domain of multi-trophic and changing ecological communities. Journal of Theoretical Biology **450**, 30–36 (2018).

29. L. G. Cosmo, et al., Indirect effects shape species fitness in coevolved mutualistic networks. Nature **619**, 788–792 (2023).

30. J. Bascompte, A. Ferrera, "A structural theory of mutualistic networks" in Theoretical Ecology, (Oxford University Press, 2020).

31. M. Dougoud, L. Vinckenbosch, R. P. Rohr, L.-F. Bersier, C. Mazza, The feasibility of equilibria in large ecosystems: A primary but neglected concept in the complexity-stability debate. PLOS Computational Biology **14**, e1005988 (2018).

32. C. Payrató-Borràs, C. Gracia-Lázaro, L. Hernández, Y. Moreno, Beyond the aggregated paradigm: phenology and structure in mutualistic networks. J. Phys. Complex. **5**, 025013 (2024).

33. S. Saavedra, R. P. Rohr, M. A. Fortuna, N. Selva, J. Bascompte, Seasonal species interactions minimize the impact of species turnover on the likelihood of community persistence. Ecology **97**, 865–873 (2016).

34. V. H. W. Rudolf, The role of seasonal timing and phenological shifts for species coexistence. Ecology Letters **22**, 1324–1338 (2019).

35. F. Duchenne, R. O. Wüest, C. H. Graham, Seasonal structure of interactions enhances multidimensional stability of mutualistic networks. Proceedings of the Royal Society B: Biological Sciences **289**, 20220064 (2022).

36. R. Ramos–Jiliberto, P. M. de Espanés, M. Franco–Cisterna, T. Petanidou, D. P. Vázquez, Phenology determines the robustness of plant–pollinator networks. Scientific Reports **8**, 14873 (2018).

37. S. Patel, M. H. Cortez, S. J. Schreiber, Partitioning the Effects of Eco-Evolutionary Feedbacks on Community Stability. The American Naturalist **191**, 381–394 (2018).

38. A. Pascual-García, U. Bastolla, Mutualism supports biodiversity when the direct competition is weak. Nat Commun **8**, 1–13 (2017).

39. R. M. May, Will a Large Complex System be Stable? Nature **238**, 413–414 (1972).

40. M. Henry, G. Rodet, Controlling the impact of the managed honeybee on wild bees in protected areas. Scientific Reports **8**, 9308 (2018).

41. R. J. Warren II, I. Giladi, M. A. Bradford, Competition as a mechanism structuring mutualisms. Journal of Ecology **102**, 486–495 (2014).

42. J. H. Ness, W. F. Morris, J. L. Bronstein, Integrating quality and quantity of mutualistic service to contrast ant species protecting Ferocactus wislizeni. Ecology **87**, 912–921 (2006).

43. A. E. Bennett, J. D. Bever, Trade-offs between arbuscular mycorrhizal fungal competitive ability and host growth promotion in Plantago lanceolata. Oecologia **160**, 807–816 (2009).

44. T. C. Adam, S. S. Horii, Patterns of resource-use and competition for mutualistic partners between two species of obligate cleaner fish. Coral Reefs **31**, 1149–1154 (2012).

45. K. H. Macphie, A. B. Phillimore, Phenology. Current Biology **34**, R183–R188 (2024).

46. I. Scheuring, "The orgy of mutualism" as an artefact: a stage structured model of plant-pollinator and seed-dispersal systems. Abstracta Botanica **16**, 65–70 (1992).

47. J. Galeano, J. M. Pastor, J. M. Iriondo, Weighted-Interaction Nestedness Estimator (WINE): A new estimator to calculate over frequency matrices. Environmental Modelling & Software **24**, 1342–1346 (2009).

48. M. Almeida-Neto, P. Guimarães, P. R. Guimarães Jr, R. D. Loyola, W. Ulrich, A consistent metric for nestedness analysis in ecological systems: reconciling concept and measurement. Oikos **117**, 1227–1239 (2008).

49. C. F. Dormann, B. Gruber, J. Fründ, Introducing the bipartite Package: Analysing Ecological Networks. R News **8**, 4 (2008).

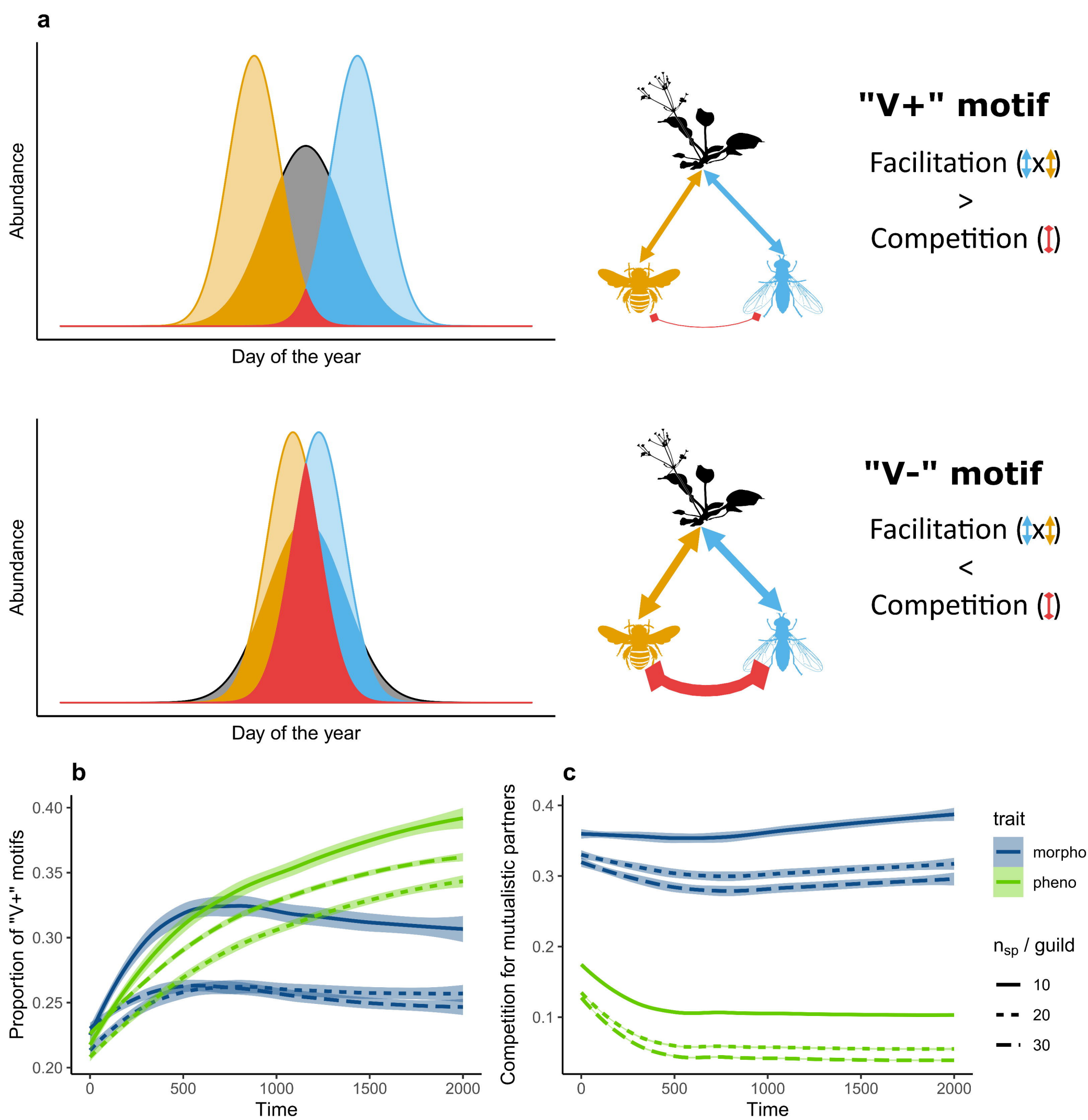
a
Abundance
Day of the year
"V+" motif
Facilitation (x)
>
Competition ()
Abundance
Day of the year
"V-" motif
Facilitation (x)
<
Competition ()
b
Proportion of "V+" motifs
0.40
0.35
0.30
0.25
0.20
0
500
1000
1500
2000
Time
c
Competition for mutualistic partners
0.4
0.3
0.2
0.1
0
500
1000
1500
2000
Time
trait
morpho
pheno
n_{sp} / guild
10
20
30

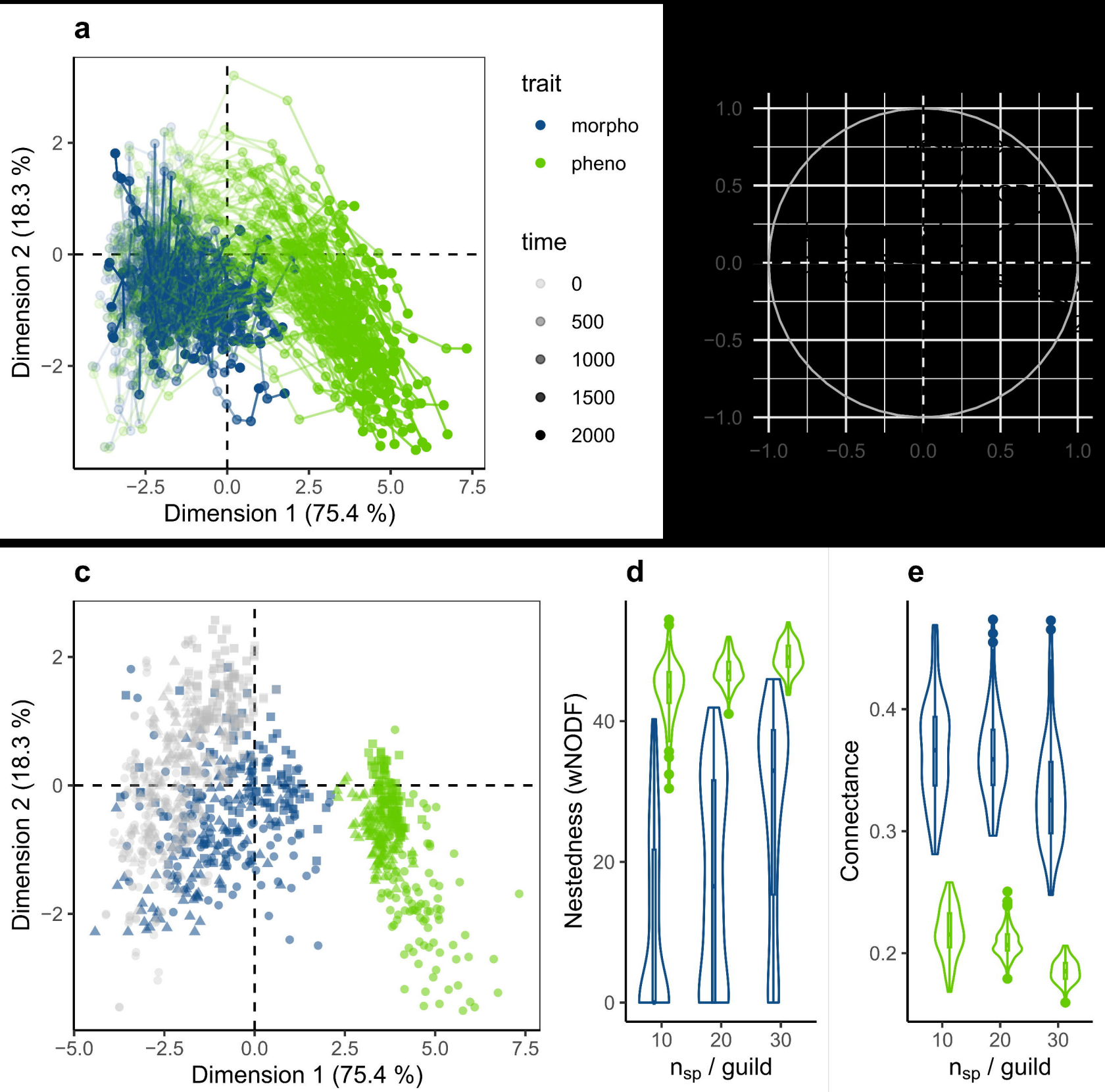
a
trait
morpho
pheno
time
0
500
1000
1500
2000
Dimension 2 (18.3 %)
Dimension 1 (75.4 %)
c
d
e
Nestedness (wNODF)
Connectance
n_{sp} / guild

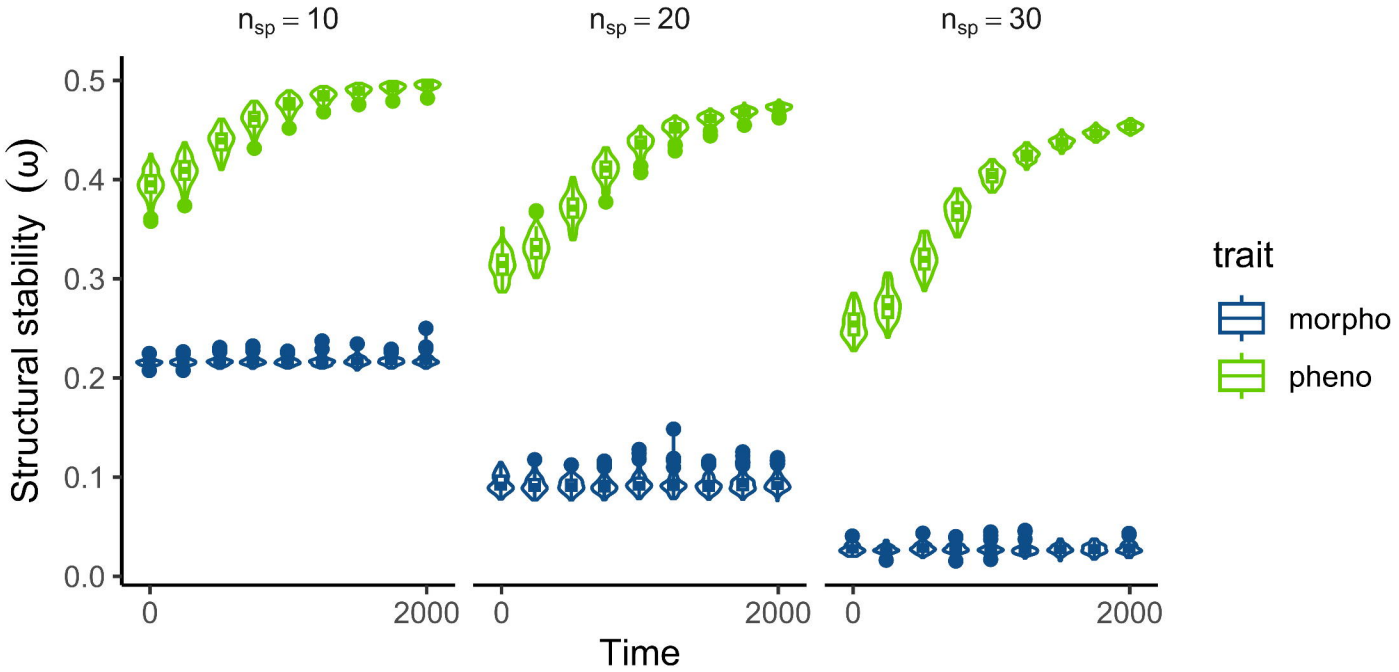
$n_{sp} = 10$
$n_{sp} = 20$
$n_{sp} = 30$
Structural stability (ω)
0.0
0.1
0.2
0.3
0.4
0.5
0
2000
Time
trait
morpho
pheno

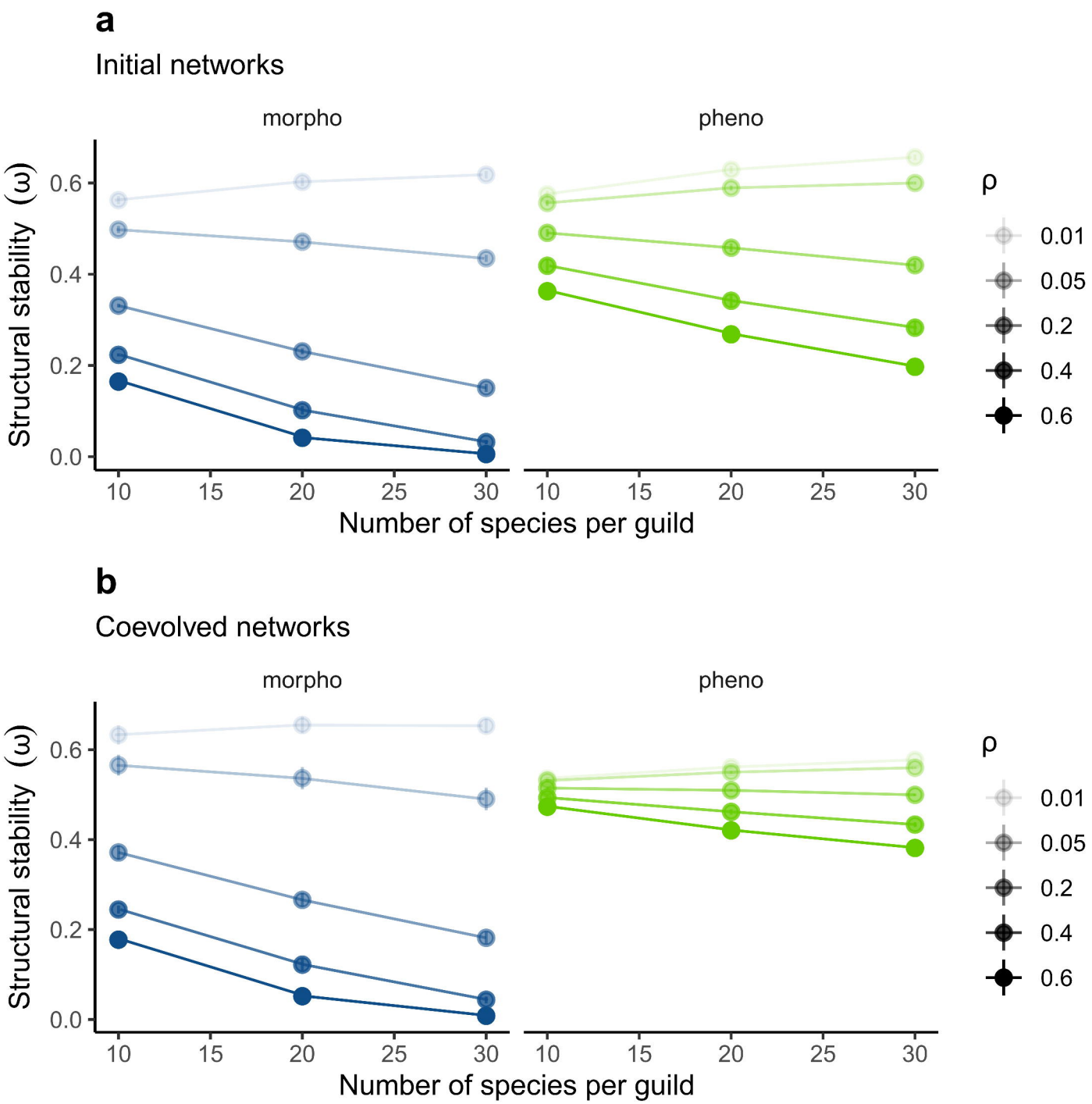
a
Initial networks
morpho
pheno
Structural stability (ω)
0.0
0.2
0.4
0.6
10
15
20
25
30
Number of species per guild
ρ
0.01
0.05
0.2
0.4
0.6
b
Coevolved networks
morpho
pheno
Structural stability (ω)
0.0
0.2
0.4
0.6
10
15
20
25
30
Number of species per guild
ρ
0.01
0.05
0.2
0.4
0.6

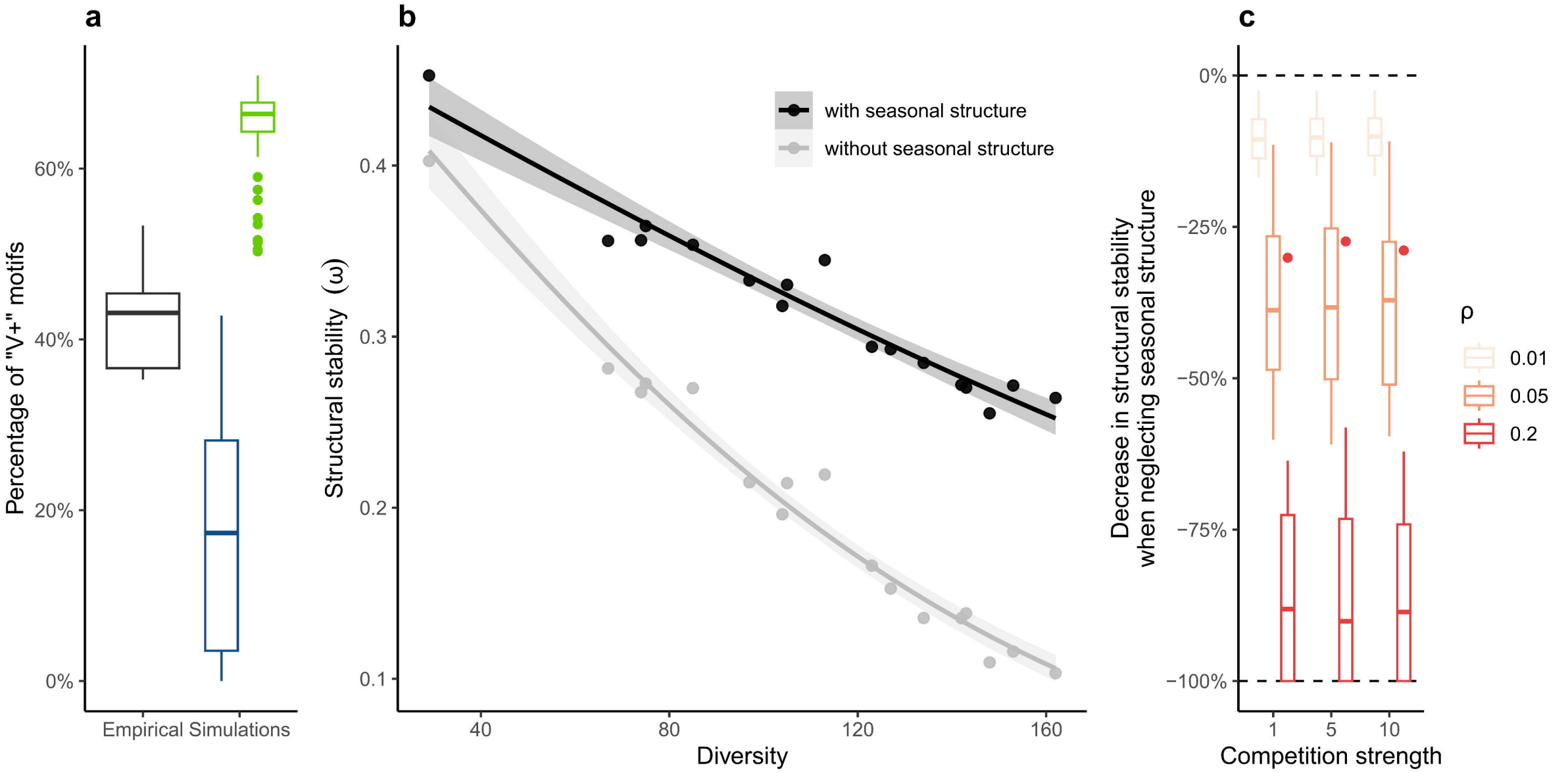
a
Percentage of "V+" motifs
60%
40%
20%
0%
Empirical
Simulations
b
Structural stability (ω)
0.4
0.3
0.2
0.1
40
80
120
160
Diversity
with seasonal structure
without seasonal structure
c
Decrease in structural stability when neglecting seasonal structure
0%
−25%
−50%
−75%
−100%
1
5
10
Competition strength
ρ
0.01
0.05
0.2